

American Crystallographic Association Single-Crystal Intensity Project Report*

BY S. C. ABRAHAMS, L. E. ALEXANDER, T. C. FURNAS, W. C. HAMILTON, J. LADELL, Y. OKAYA,
R. A. YOUNG AND A. ZALKIN†

(Received 13 May 1966)

The integrated intensity of every reflection in the (*hhl*) zone of calcium fluoride, within a radius of $\sin \theta/\lambda = 1.00 \text{ \AA}^{-1}$, has been measured diffractometrically in seven different laboratories. All participants in this project used the same ground sphere of calcium fluoride. A fixed effects analysis-of-variance model was used to investigate the seven scaled sets of structure amplitudes. Most sets contained $|F|^2$ values within five per cent of the probable true values. It is unlikely that any experiment measured $|F|^2$ values to better than two per cent. The largest systematic errors are scattering angle dependent.

Introduction

Measurement of the integrated reflection of X-rays by crystals was first made in 1913 by the Braggs. Since then, although numerous advances in technique have been recorded, the nature of the error distribution in these measurements has received relatively little attention. The recent, and now widespread, use of diffractometers for single-crystal intensity measurement, especially in automatic instruments, made a systematic study of the error in these measurements highly desirable. Accordingly, the Apparatus and Standards Committee of the American Crystallographic Association initiated the present project in June 1962.

The announced purpose of this Single-Crystal Intensity Project was 'to obtain a quantitative comparison of the absolute accuracy, and the magnitudes of the various systematic errors, in the most widely used diffractometer methods for measuring integrated intensities and resulting structure factors'.

One of the largest single sources of systematic error was eliminated by supplying each of the seven invited participants with the same standard crystal. The material chosen was calcium fluoride, on the basis of high mechanical and chemical stability, no atomic positional variables and high symmetry. A sphere of diameter $0.444 \pm 0.008 \text{ mm}$ was ground from a large single crystal of optical quality purchased from the Harshaw Chemical Company. Each laboratory was asked to measure the integrated intensity and corresponding structure factor of every reflection in the (*hhl*) zone within a radius of $\sin \theta/\lambda = 1.00 \text{ \AA}^{-1}$. In addition, the integrated intensity and structure factor of all measurable planes of the forms $\{531\}$ and $\{731\}$ were required. The radiation specified was $\text{Mo } K\alpha$. The standard crystal was mounted and oriented so that every reflection was assigned identical Miller indices by each laboratory.

* Reprints may be obtained from the Secretary of the American Crystallographic Association, Mr W. L. Kehl, Gulf Research & Development Co., P.O. Box 2038, Pittsburgh, Pa. 15230, U.S.A.

† Members of the American Crystallographic Association Single Crystal Intensity Project.

The seven participating laboratories completed the series of measurements on the crystal within ten months. The mounted standard crystal was hand-carried between laboratories. It is instructive to note that the crystal orientation, in the process of approximately 7000 miles of travel, did not change by more than about five minutes of arc.

Experimental procedures

The most important of the various experimental variables characterizing the use of the seven participating diffractometers are presented in Table 1. The stability values given in the second and third rows are defined as $100(I_{\max} - I_{\min})/I_{\text{mean}}$, where the *I*-values are integrated intensities of a given reflection measured repeatedly in the time interval stated. The large value for experiment 3 was associated with a degradation in detector resolution* from 33 to 49%. The means by which 'monochromatization' was attempted is indicated in the fourth row. The fifth row gives the technique used to reduce the count rate to within the linear range of the detector (in experiments 1, 2, 5, 6 and 7) or to correct the apparent count rate for losses. Experiment 3 used an experimentally determined table of true *versus* recorded count rate, and in experiment 4, μ , b_1 and b_2 are, respectively, the resolving time and the angle-scale half-widths of the α_1 and α_2 components of the integrated reflection. The maximum count rate used in each experiment is given in the sixth row. The term '4-circle' in the seventh row indicates an instrument in which the angles φ , χ , ω and θ may be varied, allowing all measurements to be made in the equatorial plane: 'equi-inclination' indicates variation of ω and ν only within a reciprocal lattice layer. In the eighth row, B_1 and B_2 are the extreme positions of the scan made across the reflection for experiments 1, 4, 5 and 7; in experiment 5, the count at B_1 and B_2 was measured both with balanced α - and β -foils. For experiments 1, 4 and 5, *t* is the ratio of total measurement time

* Defined as the ratio of energy spread in the pulse amplitude distribution at half maximum amplitude to the energy at maximum amplitude.

to that used at B_1 and B_2 , and in 6 to that used at B . In experiment 6, the background was measured at the position B , about 1° higher in θ than the peak position; experiment 7 is similar, except for short 2θ scans made at B_1 and B_2 and an additional scan range correction applied from an experimentally determined plot of 2θ versus dependence of apparent net intensity on scan range. This correction never exceeded 7%. In experiment 2, the first and last 3 of the 24 points at which the reflection was sampled were taken as background: in experiment 3, five points of the plateau on either side of the difference ($\beta - \alpha$) profile formed the background. The method of sampling the reflection is given in the ninth row and the complete expressions for deriving the integrated intensity in the final row. The integrated intensities were reduced to structure factors by use of the appropriate geometrical factors: absorption corrections were made in all experiments, using the mass absorption coefficients given in *International Tables for X-ray Crystallography* (1962), together with the diameter of the primary sphere previously quoted. No corrections for extinction were made in deriving the $|F|^2$ values used in the following analysis.

In addition to the primary standard crystal, which was measured by every participating laboratory, each participant was also supplied with a secondary standard sphere of calcium fluoride. The diameters of the secondary spheres ranged from 0.458 ± 0.005 to 0.517 ± 0.007 mm. These spheres were also ground from a large, optical grade, Harshaw Chemical Company single crystal. Each laboratory was asked to measure the same set of reflections, using their secondary standard, as for the primary crystal.

Statistical analysis of the data

The first step in the data analysis was to put all the data on a common scale, for no experimenter was asked to make *absolute* intensity measurements. Thus, in the final analysis all that can be determined are differences in the *relative* intensities. The scaling was performed by the method of Hamilton, Rollett & Sparks (1965), which attributes as much as possible of the discrepancy between experiments to the difference in scale factors.

A fixed effects analysis-of-variance model was then used to investigate the scaled data; the mathematical details will be found in the Appendix. The observations were classified by the following attributes: the experiment number E , the integrated intensity I , the scattering angle A , the crystal number C , and the particular member of an equivalent set of reflections F . The intensity range and the angle range were broken down into four and six levels respectively, as indicated in Table 2.

For each reflection, the scaling program also calculated the average value $|F|_{av}^2$ and the weighted deviation from the average $(|F|^2 - |F|_{av}^2)/\sigma$. It is this latter quantity which was used as the observation for the

Table 1. *Experimental variables in the participating diffractometer techniques*^(a)

	1	2	3	4	5	6	7
Experiment	1	2	3	4	5	6	7
Short term stability	1.1% (1 hour)	4.4% (30 min)	0.8% (90 min)	1.3% (1 hour)	1.0% (1 hour)	0.6% (1 min)	1.0% (1 hour)
Long term stability	1.6% (1 week)	4.4% (11 hours)	6.2% (2 weeks) ^(c)	1.3% (1 day)	1.0% (2 days)	2.3% (1 day)	1.0% (1 week)
Monochromaticity	Nb-filter	Zr-filter	Zr, Y balanced filters	Si(111) crystal reflection	Zr, Y balanced filters	Zr-filter	No filter, Zr-filter
Linearity	Nb-attenuators ^(b)	Ni-attenuators	Tabular interpolation correction	$1 + \frac{2\mu I}{27} \left(\frac{1}{b_2} + \frac{4}{b_1} \right)$ correction	Al-attenuators	No attenuator	Al-attenuators
Max count/sec	6,000	2,000	58,000	30,000	10,000	20,000	10,000
Geometry	4-circle	4-circle	Equi-inclination	Equi-inclination	4-circle	4-circle	4-circle
Background	Scan range extremes at B_1, B_2	First and last three C_j	Five point plateaus at α - and β -edges, B_1, B_2	Scan range extremes B_1, B_2	Scan range extremes $B_{1\alpha, \beta}, B_{2\alpha, \beta}$	B , at high angle side off peak	2θ scans at scan range extremes, B_1, B_2
Sampling	Continuous	Stepped $\omega, 2\theta$	Stepped ω	Simulated continuous, ω	Continuous $\omega, 2\theta$	Fixed crystal, fixed counter	Continuous $\omega, 2\theta$
Integrated intensity	$C_T - f(C_{B_1+B_2})$	$\int_{B_1}^{B_2} C_j$	$\int_{B_1}^{B_2} C_j - (B_2 - B_1) / 10 \left(\frac{B_1+B_2}{B_1} \sum_{B_2-5}^{B_2} C_j + \sum_{B_2-5} C_j \right)$	$C_T - f(C_{B_1+B_2})$	$\int_{B_1}^{B_2} C_j$	$C_{Peak} - f(C_B)$	$C_T - f(C_{B_1+B_2}) + SRC^{(d)}$

(a) All experiments used a NaI:TI scintillation crystal, photomultiplier detector. Nos. 1 and 6 used full wave rectification, all others used constant potential generation.

(b) A 9-filter pack was used for (022) and (111), with possible calibration error in attenuation factors.

(c) Associated with degradation in detector resolution during experiment, see text.

(d) Scan range correction, see text.

$$\int_{B_1}^{B_2} C_j - 4 \left(\int_{B_1}^{B_2} C_j + \sum_{B_2-22}^{B_2-24} C_j \right)$$

$$\int_{B_1}^{B_2} C_j - (B_2 - B_1) / 10 \left(\frac{B_1+B_2}{B_1} \sum_{B_2-5}^{B_2} C_j + \sum_{B_2-5} C_j \right)$$

$$C_T - f(C_{B_1+B_2}) - f(C_{(B_1+B_2)\beta}) - C_{(B_1+B_2)\alpha}$$

Table 2. Levels for classification of data according to angle and intensity

N is the number of reflections in each range. All intensity measurements are on the same arbitrary scale.

Level	$\sin \theta$	N	Level	Intensity	N
1	0.1-0.2	3	1	0-500	10
2	0.2-0.3	4	2	500-1000	15
3	0.3-0.4	7	3	1000-2000	11
4	0.4-0.5	7	4	2000	9
5	0.5-0.6	8			
6	> 0.6	16			

analysis-of-variance. If the weights were properly chosen, the random errors of observation e should be identically distributed. Two weighting schemes were used: in the first set, $\sigma(|F|^2) = 0.02 |F|^2$; in the second set, $\sigma(|F|^2) = (|F|^2)^{\frac{1}{2}}$. The latter scheme would be identical with a weighting based on counting statistics if the Lorentz-polarization factors were all equal. The complete analyses were carried out with both weighting schemes; there were no differences in the conclusions. Since a detailed examination of the weighted residuals indicated that the first weighting scheme was preferable, the numerical results are quoted for that scheme only.

A preliminary analysis, and also the experience of the experimenters, indicated that there were systematic differences between the primary and secondary crystals. The crystals used were subject to severe extinction, so the differences between crystals could probably be attributed to differences in size and possibly in the mosaic character. Since differences between crystals could obscure other effects of interest, subsequent analyses were carried out on the primary crystal only. The ratio $R = (|F|_P - |F|_S) / \frac{1}{2}(|F|_P + |F|_S)$ is presented in Table 3 for the five experimenters who measured both the primary (P) and a secondary (S) crystal.

Table 3. R ratios between primary and secondary crystals

Experiment	R (based on F)
1	0.020
2	0.034
3	0.107
6	0.086
7	0.053

Various members of the {731} form and of the {531} form were measured by six of the seven experimenters. Most measured 24 of the possible 48; each of the 48 however was observed by at least two experimenters. The hypothesis tested in each case was

H_0 : All members of the form are equal in intensity. This hypothesis could not be rejected either for {731} or {531} at the 0.05 significance level. This implies that for a given member of the form, the agreement among the experimenters was no better than the agreement for all members of the form for a single experimenter. The results (with $|F|$ on an arbitrary scale) are presented in Table 4. There is no evidence from the data summarized in Table 4, or from the other measurements

Table 4. Summary of data on comparison of equivalent reflections

	{731}	{531}
Range in $ F $	685-706	788-824
Mean (μ)	697	804
$\sigma(\mu)$	11	14
$\sigma(\mu)/\mu$	0.016	0.017
F ratio	1.086	1.22

$F_{48,82,0.05} = 1.5$. Hypotheses not rejected.

made, that any reflection was in serious error owing to systematic multiple diffraction.

Because any differences in intensity for various members of a form seemed to be less than other errors in the measurements, in the final analysis the indices of all reflections were made positive and permuted so that $|h| \leq |k| \leq |l|$. For any one experimenter, all equivalent reflections were averaged together with any reflection that had been measured more than once. Thus for each hkl , each experimenter was represented but once. These data were rescaled and subjected to an analysis-of-variance using the following fixed-effects model:

$$(|F_{ijkn}|^2 - |F_{av}|^2) / \sigma = y_{ijkn} = \mu + \mu^E_i + \mu^I_j + \mu^A_k + \mu^{EI}_{ij} + \mu^{EA}_{ik} + e_{ijkn} \quad (1)$$

The discrepancies between experiments, for the three reflections in the first angle level, seemed unexpectedly large. Two analyses were carried out, one including this group of reflections, another omitting it. The conclusions were the same for both treatments; it is the latter treatment which is reported.

The following hypothesis tests were made:

H_0 : The experiment-angle interaction terms μ^{EA}_{ik} are equal. $F_{24,194} = 4.626^*$.

The hypothesis may be strongly rejected;

$$F_{24,194,0.005} = 2.0.$$

H_0 : The experiment-intensity interaction terms μ^{EI}_{ij} are equal. $F_{18,194} = 1.52$.

The hypothesis cannot be rejected at the 0.05 significance level since $F_{18,194,0.05} = 1.6$.

The rejection of the first hypothesis means that there are probable systematic errors in one or more of the experiments which are angle-dependent. In any one angular range, the experiments (if scaled to that range) would agree better than they do overall. The estimated effects $\mu^E + \mu^A + \mu^{AE}$ are plotted in Fig. 1 against angle. In viewing Fig. 1 and Fig. 2, it is important to note that only differences between effects have meaning. For example, experiment 1 shows a smooth increase in intensity with angle as compared with experiment 2. The fact that the curve for experiment 2 is more nearly horizontal does not imply that it is more nearly 'correct'. Either one could be closer to the truth. We do know that a refinement of the structure would lead

* $F_{m,n}$ is the variance ratio for m (dimension of the hypothesis) and n (difference between number of observations and variables) degrees of freedom.

to larger thermal parameters for experiment 2. Similarly, the origins of the curves are arbitrary; they could, for example, be adjusted to agree perfectly at either low or high angles; it is only the difference in shape as a function of angle that is important.

Fig. 2 shows the effects plotted against intensity for the several experiments; as noted above, there are no significant systematic differences.

The largest discrepancies in intensity as a function of angle appear in comparing experiment 6 with the other experiments. Experiment 6 shows a uniform decrease in intensity compared with the others as the scattering angle increases. It is possible that in this particular application of the stationary-crystal stationary-counter technique, all of the diffracted intensity was not reaching the counter aperture at the higher angles.*

Table 5 presents the interexperiment R ratios based on $|F|^2$. It is interesting to note the exceptionally good agreement between experiments 2, 4, 5, and 7.

Table 5. Interexperiment R ratios based on $|F|^2$

$$R = (|F|_i^2 - |F|_j^2) / \frac{1}{2}(|F|_i^2 + |F|_j^2)$$

Primary crystal only.

	1	2	3	4	5	6	7
1	0.084	0.122	0.083	0.076	0.126	0.061
2		0.061	0.025	0.020	0.101	0.039
3			0.068	0.055	0.107	0.064
4				0.021	0.107	0.031
5					0.103	0.032
6						0.089

Conclusions

1. The agreement between the experiments is good. The possibility that routine data collection can produce $|F|^2$ values which may be within 5% of the true values has not been fully exploited.
2. There is no evidence that any experiment is measuring $|F|^2$ values to better than 2%.
3. The largest systematic errors revealed in this study are those associated with scattering angle. This is illustrated not only by the large F ratio but by the nicely systematic trends in Fig. 1. These are the types of errors which can be, and probably often are, absorbed in temperature factors in crystal structure refinements. This would suggest that the absolute magnitudes of many thermal parameters in the literature should be regarded with suspicion (examples are given by Abrahams, 1965), despite the fact that low R values have been obtained. Note however that the maximum effects observed here would only represent a change of B of about 0.3 \AA^2 .
4. It seems unlikely that anisotropy of crystalline perfection introduces errors of more than 2% in $|F|^2$ for the standard sphere of calcium fluoride. Such errors have not been demonstrated in the present experiment.

* An analysis omitting experiment 6 was also carried out. There were still highly significant experiment-angle interactions among the other six experiments.

5. Differences in perfection and crystal shape may cause substantial error between crystals if the extinction is high. This may represent one of the largest sources of error in practical work.

6. Since each experimental technique was used only once, no measure of possible differences between techniques and, or, instruments as opposed to differences between investigators is available.

7. Further experiments at a lower significance level are necessary in order to give a clearer separation of errors inherent in the different techniques. An extension of the scattering angle range is also necessary to obtain maximum information on those errors that are systematic with angle.

APPENDIX

The results were analyzed by conventional analysis-of-variance techniques, which we summarize briefly. Consider that the observation of a quantity y may be clas-

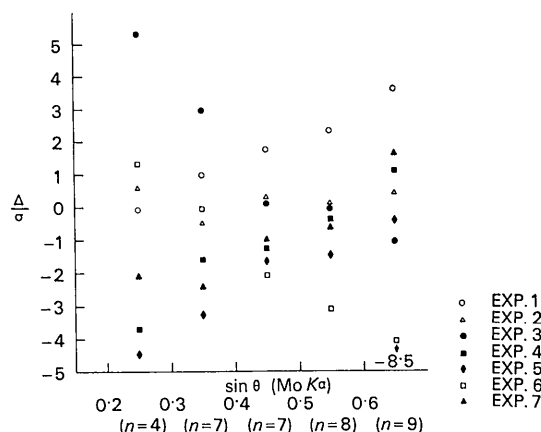


Fig. 1. Estimated experiment-angle interaction effects in the analysis-of-variance of the experimental data. Only the relative differences are meaningful. The points close to zero are not necessarily better than other points; they are only closer to the average. n is the number of independent reflections in each interval of $\sin \theta$. $\Delta/\sigma = \mu + \mu^{E_i} + \mu^{A_k} + \mu^{E_{ik}}$.

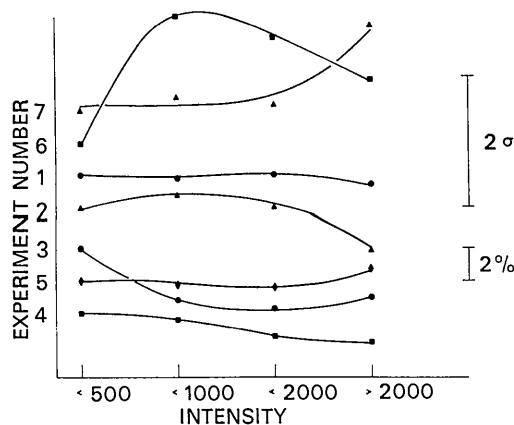


Fig. 2. Estimated experiment-intensity interaction effects. The error bar indicates the standard deviation of any one of these estimates. It can be seen that there are no significant trends. The origins for the various experiments have been displaced by an arbitrary amount.

sified according to two attributes *A* and *B*, each of which may take on several discrete values, commonly called *levels*. Associated with the level A_i we may define an *effect* μ^{A_i} ; if an observation belonging to the *i*th level of *A* is, on the average, larger in magnitude than one in the *k*th level of *A*, we say that the effect μ^{A_i} is greater than the effect μ^{A_k} . If we further define an interaction effect $\mu^{AB_{ij}}$ and a random error of measurement, e_{ijn} , we may write the *n*th observation in the *i*th class of *A* and the *j*th class of *B* as

$$y_{ijn} = \mu + \mu^{A_i} + \mu^{B_j} + \mu^{AB_{ij}} + e_{ijn} \quad (A1)$$

μ is the mean value of *y* if all effects are zero, since e_{ijn} is defined to have zero mean; for the purposes of

hypothesis testing, it is assumed further that all the e_{ijn} have identical normal distributions.

The analysis-of-variance procedure involves a least-squares estimation of the values of the parameters μ , μ^{A_i} , μ^{B_j} , $\mu^{AB_{ij}}$.*

The least-squares estimation is carried out both when the parameters are constrained by a linear hypothesis H_0 and when they are unconstrained. The hypotheses will usually specify that certain parameters are equal or zero. For example, one might wish to test

* It is important to note that a unique least-squares solution does not exist for all the parameters in equation (A1). There are constraints which allow one only to estimate *differences* in effects and not the absolute magnitudes of the effects.

Table 6. $|F|^2$ for various experiments on arbitrary scale
Uncorrected for extinction

			Experiment						
<i>h</i>	<i>k</i>	<i>l</i>	1	2	3	4	5	6	7
0	0	2	4.5	5.1	5.5	4.5	4.6	6.5	-----
0	0	4	850.7	852.6	913.0	824.6	842.8	962.4	-----
0	0	6	77.7	75.5	79.2	74.6	74.0	89.4	72.4
0	0	8	450.4	425.1	409.9	424.2	423.3	462.8	414.4
0	0	10	52.0	49.0	47.3	49.4	46.1	-----	50.5
0	2	2	663.4	1040.5	1086.3	1009.4	1035.3	859.9	890.3
0	4	4	679.3	633.9	698.2	649.0	666.0	585.3	653.3
0	6	6	398.9	372.6	370.8	384.7	379.4	325.8	378.8
0	8	8	-----	178.1	-----	189.4	-----	-----	-----
1	1	1	314.1	486.2	578.3	477.0	501.4	519.9	-----
1	1	3	462.3	465.0	497.7	443.4	465.5	538.9	475.0
1	1	5	376.0	357.0	363.6	363.5	362.3	429.1	370.5
1	1	7	284.3	278.5	260.0	267.2	270.9	296.9	265.3
1	1	9	187.9	176.8	172.0	179.9	178.2	183.2	181.2
1	1	11	-----	98.1	-----	105.1	-----	-----	-----
1	3	3	423.9	396.8	458.2	389.6	414.9	386.6	413.2
1	3	5	330.8	321.1	327.1	324.2	328.5	358.2	-----
1	3	7	244.5	247.3	235.0	242.5	244.3	255.3	-----
1	5	5	279.5	277.4	269.6	268.1	280.2	245.1	264.9
1	7	7	150.6	144.5	137.8	144.0	143.0	114.1	144.8
2	2	2	41.3	43.4	45.3	39.0	38.8	47.0	40.0
2	2	4	719.0	697.8	729.9	701.4	719.7	777.0	713.1
2	2	6	81.2	78.8	76.3	76.1	77.1	89.5	77.6
2	2	8	396.8	376.2	360.9	377.3	380.3	395.7	378.2
2	2	10	46.4	42.6	41.9	44.1	43.4	-----	45.5
2	4	4	78.6	76.7	79.5	74.9	73.9	74.3	74.9
2	6	6	67.8	67.1	63.6	64.6	62.8	57.4	-----
2	8	8	-----	30.3	-----	32.1	-----	-----	-----
3	3	3	362.1	356.5	381.1	351.6	360.0	382.8	364.8
3	3	5	302.1	294.7	278.4	290.7	291.1	321.5	288.2
3	3	7	228.9	225.9	216.0	217.2	218.2	238.3	217.4
3	3	9	150.5	138.6	137.0	142.4	143.6	132.4	143.4
3	5	5	254.7	245.6	240.1	242.7	242.7	232.9	239.8
3	7	7	-----	132.0	-----	128.8	131.0	-----	-----
4	4	4	522.8	497.7	483.4	507.4	523.4	510.3	495.1
4	4	6	73.0	69.6	68.8	68.1	68.8	71.6	68.6
4	4	8	285.8	268.4	256.7	277.7	273.2	249.9	276.5
4	4	10	-----	29.0	-----	30.2	-----	-----	-----
4	6	6	315.1	305.4	237.2*	304.2	303.4	263.0	307.0
5	5	5	202.4	194.4	189.9	192.4	193.2	182.2	194.3
5	5	7	152.5	147.8	141.5	145.8	145.8	129.8	146.9
5	5	9	-----	85.3	-----	91.7	-----	-----	-----
5	7	7	-----	98.5	-----	102.2	-----	-----	-----
6	6	6	45.9	42.1	43.5	43.8	42.4	35.6	43.6
6	6	8	-----	149.1	-----	171.4	-----	-----	-----

* At the proof stage this magnitude, which was used throughout the analysis, was found to be incorrectly transcribed from the original value of 293.2.

whether all interaction effects are zero or whether all levels of A have the same effect. A decision on whether to reject the hypothesis is based on examination of the ratio of the goodness-of-fit parameter for the two least-squares estimates; this ratio is tested as the usual variance ratio F .

The actual calculations were carried out by a general computer program HANOVA, available on request from WCH. A further discussion of the model may be found elsewhere (Hamilton, 1964, for example.)

The experimental contributions of J. L. Bernstein, K. Knox, N. R. Stemple and P. Mackie to various parts of this project are gratefully acknowledged. The work

of some of the participating laboratories was supported by the National Science Foundation (Contract no. GP3864), the United States Atomic Energy Commission and the National Institutes of Health—National Institute of Dental Research (Grant no. DEO1912-04).

References

- ABRAHAMS, S. C. (1965). *Acta Cryst.* **18**, 926.
 HAMILTON, W. C. (1964). *Statistics in Physical Science*. New York: Ronald Press.
 HAMILTON, W. C., ROLLETT, J. S. & SPARKS, R. A. (1965). *Acta Cryst.* **18**, 129.
International Tables for X-Ray Crystallography (1962). Vol. III, p. 164. Birmingham: Kynoch Press.

Acta Cryst. (1967). **22**, 6

Small-Angle X-ray Scattering by Rods and Sheets: The Interpretation of Line-Collimation Results

BY R. E. BURGE AND J. C. DRAPER

Department of Physics, University of London, Queen Elizabeth College, Campden Hill Road, London W8, England

(Received 6 April 1966 and in revised form 21 June 1966)

The conditions are examined under which direct interpretation is possible of small-angle intensity data for isotropic solutions of long rods and thin discs collected with the use of infinite line collimation conditions and on an absolute scale. It is shown by extensive computer calculations, using five different rod models and three different disc models, that in all cases where data obtained under point collimation conditions can be unequivocally interpreted (*i.e.* free of dependence on a theoretical model) in terms of the number of electrons per unit length (area) of rods (discs) and the appropriately defined radius of gyration, the very small-angle infinite line collimation results can be used directly to give the same information.

The effects of the finite length of rods and finite area of discs are considered and the conditions analysed where the measured scattering may be interpreted as if the rods were very long and the discs were of very large area.

Introduction

Kratky and co-workers and Luzzati and co-workers (for reviews see Kratky, 1963; Luzzati, 1963) have discussed the small-angle X-ray scattering method as applied to macromolecular solutions where the intensity of scattering is assessed on an absolute scale, *i.e.* relative to the energy of the incident beam.

The intensity of X-rays scattered by a dilute, isotropic, macromolecular solution depends on the cross-section of the X-ray beam at the specimen. Cases that have been considered are point collimation and both finite and infinite line collimation (for references see Chu & Creti, 1965). Scattering results are normally obtained with slit collimation and for the purposes of interpretation the results are corrected back to point focus conditions by numerical methods. Luzzati (1958, 1960), however, showed that results obtained with the use of infinite line focus conditions at the specimen

could, for spherical and rod-like particles, be interpreted directly. It was decided in the present work to examine further the direct interpretation of infinite line-focus data from rods and to consider sheets also because of work in progress in this laboratory on bacterial flagella and bacterial cell walls.

Luzzati (1960) interprets the scattering by rods under line collimation conditions by using a rod-model with a given distribution of electron density perpendicular to the rod axis and by evaluating the differences between the predictions of the model and the experimental results. It is not clear in the formulation of the problem as used by Luzzati (1960), first how far the physical parameters deduced for the rods reflect the model used and, second, whether to interpret line-collimation results on the basis of any other rod model makes mandatory their conversion into data appropriate to point collimation conditions. The calculations reported here are addressed to these two problems in